

---

## CHARACTERIZATION OF ZINC OXIDE NANOPARTICLES PREPARED BY SONOCHEMICAL METHOD WITH DIFFERENT ULTRASONIC EXPOSURE POWER

---

M. Ashoush<sup>1</sup>, L.M. Alsaba<sup>2\*</sup>, A. Eid<sup>4</sup>, S.N. Elsayed<sup>3</sup>, Asmaa. Abdelghany<sup>4</sup>.

(1) Faculty of Science, Al-Azher University, Cairo, Egypt.

(2) Higher Technological Institute (HTI), 6<sup>th</sup> October Branch, 6<sup>th</sup> October City, Egypt

(3) National Institute of Standards, Tersa st, Giza, Egypt

(4) Faculty of Science, Al-Azhar University, Girls Branch, Cairo, Egypt.

\* Corresponding Author: [lalsabaphysics@gmail.com](mailto:lalsabaphysics@gmail.com).

---

### ABSTRACT

In the present study ZnO nanoparticles have been synthesized using sonochemical technique at different ultrasonic exposure power. The powers were 20%, 40% and 60% of the total power of ultrasonic generator (operating at 20 kHz with a maximum power output of 250 W). The experimental procedures were carried out in Ultrasonic Lab, National Institute for Standards, Egypt. ZnO nanoparticles samples were investigated by X-ray diffraction (XRD), Transmission Electron Microscope (TEM), UV visible Absorption and Fourier Transform Infrared Spectroscopy (FTIR). XRD and TEM results reveal that Exposure power has a pronounced effect on both particle size as well as morphology. The greater the exposure power, the larger the particle size. In addition, the morphology of ZnO nanoparticles modified from rod-like shape to semi-spherical shape by raising the exposure power. The band gap for all samples estimated by UV absorption data was found to be around 3.1 eV. The ZnO absorption band was observed at 560 cm<sup>-1</sup> in FTIR spectra.

**Key words:** sonochemical method, exposure power, crystalline size.

### 1. INTRODUCTION

Zinc oxide semiconductor with wide band gap ( $E_g = 3.37$  eV) and a high exciton binding energy (60 meV) at room temperature and excellent chemical stability [1] is vastly used in many applications like photocatalysis, gas sensors, varistors, for water treatment applications, solar cells, and biomedical applications [2-9]. The particle size and morphology of particles are very important parameters in those applications so the attention is directed to prepare it in the nanoscale. ZnO nanoparticles have been synthesized by different methods such as sol-gel, precipitation, DC thermal plasma synthesis, spray pyrolysis, hydrothermal synthesis, and wet mechanical method [10-17]. In the last few years sonochemical method has been used heavily for preparing nanostructured materials [18-22]. Sonication of solutions in sonochemical method results in the formation, growth, and implosive collapse of bubbles in the liquid. This phenomenon is named cavitation. As a result of this phenomenon a very high

temperatures of 5000 °K and pressure up to 1800 atm making local hot spots. These hot spots are responsible for the reactions and the formation of nanoparticles [24-25]. The sonochemical method of preparation the ZnO nanoparticles with different particle sizes during a small period of time (only about one hour for each sample) with changing only the exposure power of the ultrasound waves with less effort and less time gives us the ability to produce more samples for using in the past interested applications. Given the increasing interest in ZnO nanoparticles as potential candidates for piezoelectric and photovoltage solar cells devices as well as UV light emitters, the present study offers a facile route towards the fabrication of finely tuned Zinc Oxide nanoparticles with cost effective and on demand sizes and morphologies.

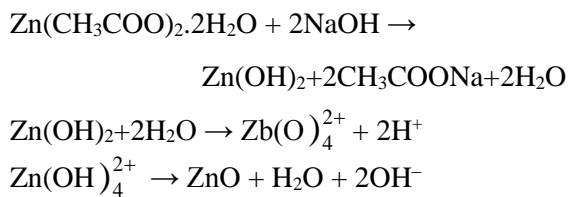
### 2. EXPERIMENT

#### 2.1. Preparation of ZnO Nanoparticles

Zinc Oxide (ZnO) nanomaterials have been synthesized sonochemically by different adjustments of powers of the ultrasound

technique which were used in the process of preparation. 12 gm of Sodium hydroxide (3M) was dissolved in distilled water and poured drop wise onto the solution of 4.38 gm (0.2 M) of Zinc Acetate dihydrate ( $(\text{Zn}(\text{CH}_3\text{COO})_2 \cdot 2\text{H}_2\text{O})$ ) under stirring by magnetic stirrer for 10 min. The suspension was ultrasonically irradiated for one hour with a high-density ultrasonic probe immersed directly into the solution at power values 20%, 40% and 60% from the total power of the sonifier (250W). The PH of the solution was maintained at 13. The solution was filtered and washed several times with distilled water and methanol to remove undesired impurities. Finally, the resultant wet powder was dried at room temperature.

The decomposition of  $\text{Zn}(\text{CH}_3\text{COO})_2 \cdot 2\text{H}_2\text{O}$  into ZnO can be described according to:



## 2.2. Structural and Morphology Measurements

X-ray diffraction patterns of the samples are recorded with Multi-purpose X-ray Diffractometer (X'Pert-MPD system) using  $\text{CuK}\alpha$  radiation ( $\lambda=0.154056$  nm) at an X-ray tube of Power 3050 W/00Cu LFF (40kV, 30mA).

Transmission electron microscope (TEM- JEOL Co., Made in Japan, with Max-Power of 600 KX, Max-Resolution of 0.2 nm, Max-Energy of 120 kV) has been used for data collection.

## 2.3. Optical Measurements

The characterization of the absorption bands of ZnO samples were performed using Fourier Transform Infrared Spectrophotometer (Shimadzu FTIR-8400 S, Japan). The optical absorption spectra of the samples were taken by UV-Vis spectroscopy. UV-Vis Absorption

measurements were carried out using double beam Spectrophotometer (Type: JASCO Corp., V-570, and Rev. 1.00).

## 3. RESULTS AND DISCUSSION

### 3.1. Structural and Morphology Measurements

#### 3.2.1. XRD Measurements

ZnO nanoparticles prepared at different exposure sonication power 20%, 40% and 60% of the total power of the sonicator system (The sonifier) will be denoted as 20, 40 and 60 respectively. XRD patterns of ZnO samples are shown in fig.1. The results reveal that all characteristic peaks of crystalline wurtzite hexagonal phase of ZnO (JCPDs, card no. 36-1451) are distinctly appeared in XRD patterns. Sharp and high intense diffraction peaks indicates the high degree of crystallinity for all samples. Diffraction peaks (marked by \*) were Barely observed for a and b samples which attributed to Zn  $(\text{OH})_2$  residuals.

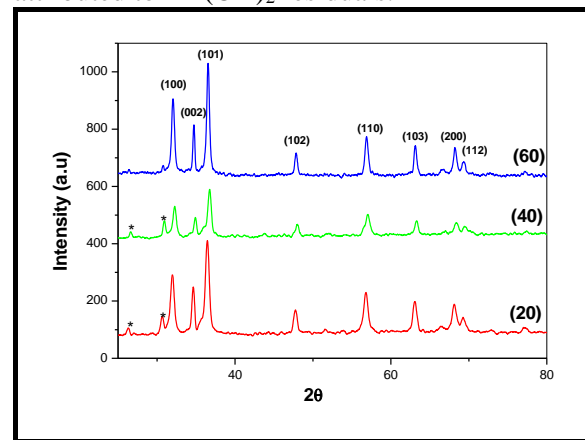


Fig. (1) XRD patterns of 20, 40 and 60 samples.

Particle size for all samples has been estimated via both well known Scherer formula [26, 27], and Williamson-Hall analysis (W.H analysis) [28], eq. 1 and 2 respectively.

$$D = 0.9 \frac{\lambda}{\beta \cos \theta} \quad (1)$$

$$\cos \theta = \frac{k \lambda}{D} + 4 \varepsilon \sin \theta \quad (2)$$

The calculated particle size of ZnO nanoparticles are listed table. 1.

**Table. 1.** Particle size calculations using for 20, 40 and 60 samples.

sample	Particle size (D) from Scherrer equation (nm)	Particle size (D) from UDM (nm)
20%	15	15
40%	17	17
60%	22	23

As shown in table.1 it is clear that there is no noticeable difference between particle size estimated by Scherrer equation and that estimated by Williamson-Hall, this is because of the negligible value of the strain. It can also be seen that the particle size of the samples increases by raising exposure power. Increasing exposure power causes the temperature of the hot spots to increase which results in the formation, growth, and implosive collapse of bubbles in the liquid to be high and increasing in particle sizes occur.

The lattice parameters of samples 20, 40 and 60 were calculated using the Lattice Geometry equations (3-5) and summarized in table 2.

$$d_{hkl} = \frac{\lambda}{2 \sin\theta} \tag{3}$$

$$\frac{1}{d^2} = \frac{4h^2 + hk + k^2}{3a^2} + \frac{l^2}{c^2} \tag{4}$$

$$V = \frac{\sqrt{3a^2c}}{2} = 0.866a^2c \tag{5}$$

### 3.1.2 TEM Measurements

Transmission Electron Microscope images taken for ZnO nanoparticles samples 20, 40 and 60 were shown in figure. 3. It is obvious that the morphology of the particles mightily influenced by exposure power. Rod like shape particles are detected for sample 20 which modified to mixture red like shape and semispherical particles for sample 40. Semispherical like shape particles are observed for sample 60 while the particles with rod like shape are completely disappeared. The results are evidence that the morphology of the nanoparticles as well the particle size can be

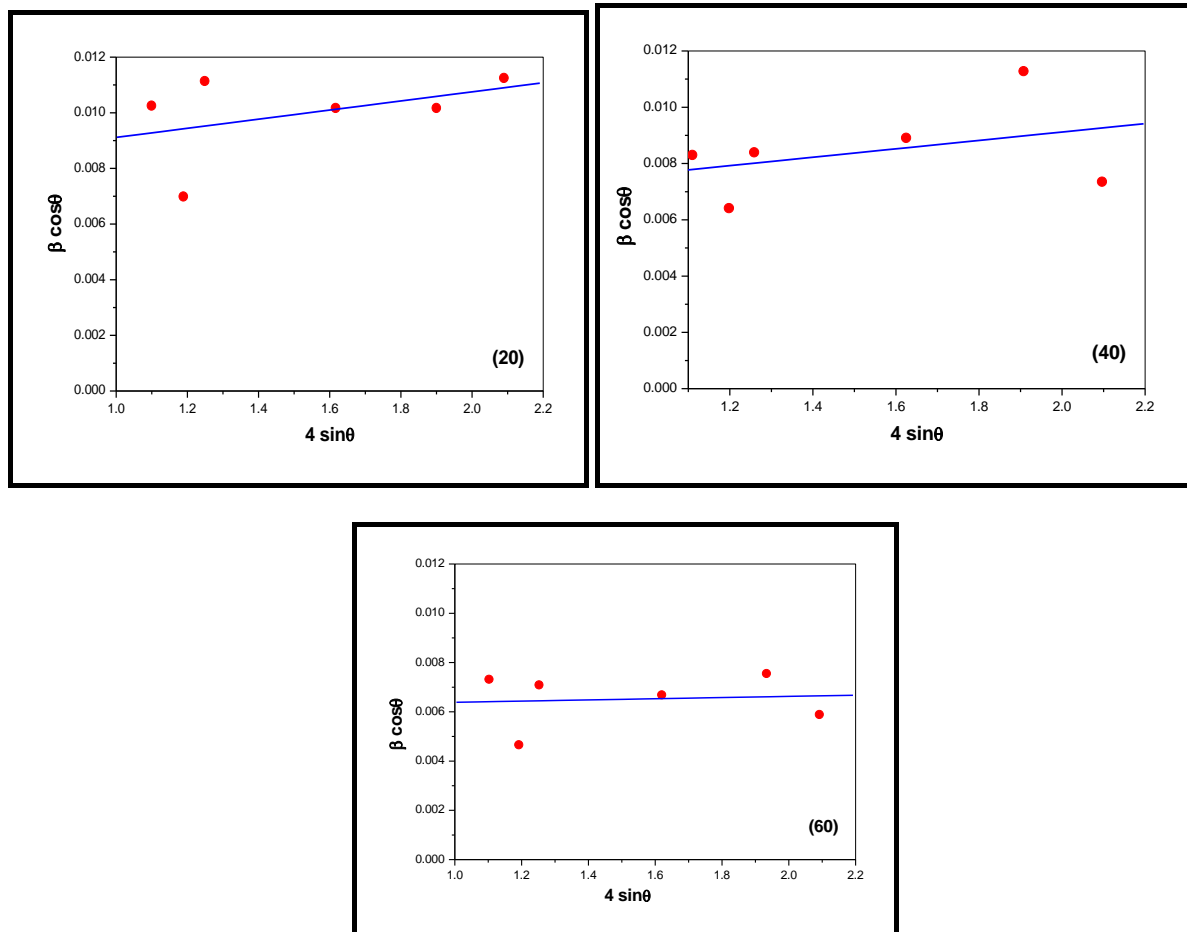


**Fig. 2.** The W-H analysis using UDM for 20, 40 and 60 samples.

controlled by the power of ultrasound waves. At higher values of power, larger particle sizes is expected and spherical shapes can be found, while the small values of powers are enough to obtain rods like shapes in the samples.

### 3.2. Optical Measurements

#### 3.2.1. Characterization of absorption bands in samples by FTIR

The FTIR measurements of samples were carried out in the range of (400- 4000  $\text{cm}^{-1}$ ). Figure 4 shows the absorption bands for 20, 40 and 60 samples.

All the observed bands and their assignments are tabulated in table 3. The absorption band located at 560  $\text{cm}^{-1}$  can be attributed to ZnO stretching mode [29-31].

The UV- visible absorption spectra of the ZnO samples are shown in figure 5. Tauc's equation [25, 26] was used to calculate the band gap values of the samples.

$$(\alpha h\nu)^{\frac{1}{n}} = A (h\nu - E_g) \quad (6)$$

Where  $\alpha$  is the absorption coefficient,  $h\nu$  is the energy of incident photon, A is constant,  $E_g$  is the optical band gap and n equal ( $\frac{1}{2}$ , 2,  $\frac{2}{3}$  or 3) depending on the type of transition. For direct transition n equal  $\frac{1}{2}$ . Figure 6 shows the relation between  $(\alpha h\nu)^2$  versus photon energy  $h\nu$ . The band gap  $E_g$  can be getting from the extrapolation of the linear portion of the curve with the energy axis ( $h\nu$ ). The optical band gap was found to be 3.1 eV for all samples which is

**Table 2:** The structural parameters of 20, 40 and 60 samples.

sample	(hkl)	Interplane spacing, d (nm)	Lattice parameter			V (nm) <sup>3</sup>
			a (nm)	c (nm)	c/a	
20	(100)	0.28	0.32	0.52	1.6	0.046
	(002)	0.26				
40	(100)	0.28	0.32	0.51	1.6	0.045
	(002)	0.26				
60	(100)	0.28	0.32	0.52	1.6	0.046

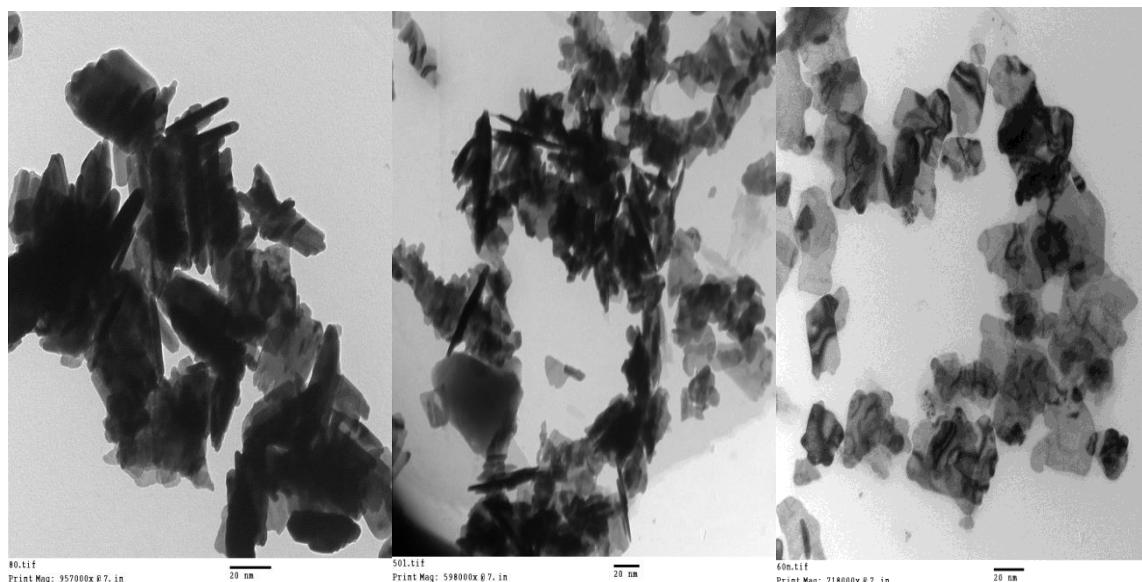


**Fig. (3):** TEM images for 20, 40 and 60 samples.

#### 3.2.2. Calculations of the band gap of ZnO nanoparticles from UV-vis measurements.

smaller than that of bulk ZnO (= 3.37 eV) reported by Berger et al [34].

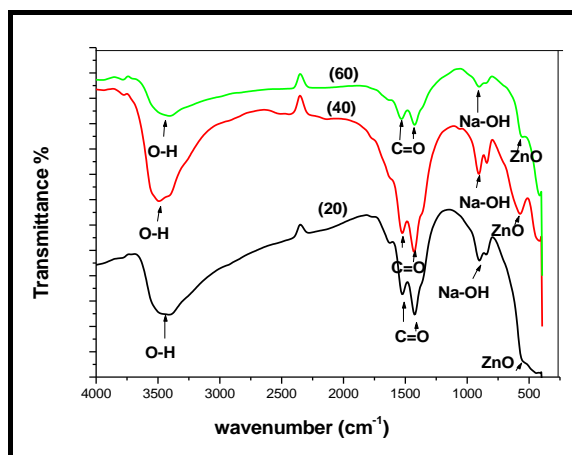


Fig. (4). FTIR for 20, 40 and 60 samples.

Table (3): Assignment for all observed FTIR peaks for 20, 40 and 60 samples.

Position $\text{cm}^{-1}$	3500-3420	1530-1510	900-830	Around 560
Assignment	O-H stretching	C=O	Na-OH	ZnO

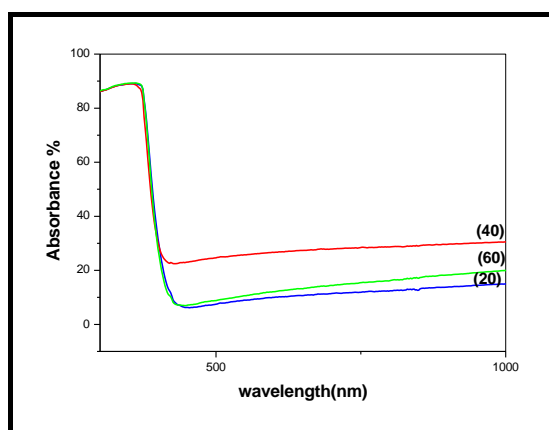


Fig.5. UV absorption spectra for 20, 40 and 60 samples.

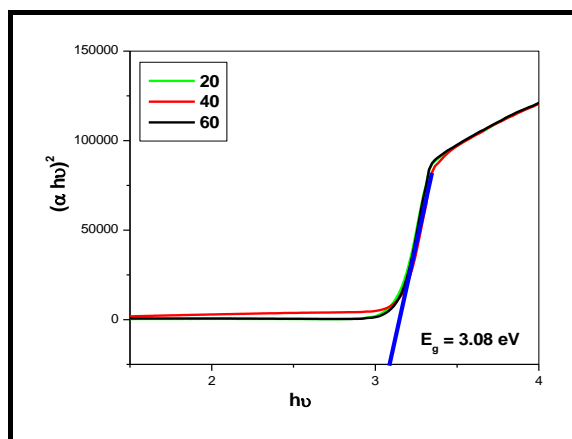


Fig.6.  $(\alpha h\nu)^2$  versus  $h\nu$  for 20, 40 and 60 samples.

## CONCLUSION

ZnO nanoparticles have been prepared by sonochemical method with different ultrasonic exposure powers of (20%, 40% and 60%) from the total power of the sonifier used in the synthesis process. The structural measurements taken by XRD and TEM showed that, the exposure power has significant influence on both particle size and morphology of the samples. The particle size was found to increase by raising the exposure power. The morphology of the particles was modified from rod like shaped for sample 20 to semispherical like shape for sample 60. FTIR curves showed the characteristic band of ZnO was seen at  $560 \text{ cm}^{-1}$ . The band gap estimated from UV measurements was found lies at about 3.1 eV for all samples which close to that of ZnO bulk.

## REFERANCES

- [1] Z.L. Wang, Nanostructures of zinc oxide, *Materials Today*, 7, (26–33), (2004).
- [2] TK. Gupta, *J. Am. Ceram. Soc.* 73, (1817), (1990).
- [3] JR. Harbour, ML. Hair, *J. Phys. Chem* 83, (652), (1979).
- [4] Mitra, P, Chatterjee, A, Maiti, H: *Mater. Lett.* 35, (33), (1998).
- [5] G. Deak, P. Ana- Maria, *INTJGONSERV SCI* 10, 2, (343-350), (2019).
- [6] B. A. Abbasi, J. Iqbal, R. Ahmad, L. Zia, S. Kanwal, T. Mahmoud, C. Wang and J.T. Chen, *Biomolecules* 10, 38, (2020).
- [7] S. Eonjin and H. Eonjin, *Pharmaceutics*, 11, 575, (2019).
- [8] H. Musleh, H. Zayed and et.al, *Egypt. J. Chem*, (111-123), Special Issue (2019).
- [9] K. Č. Barabaszova, S. Holešová and et.al, *Nanomaterials*, 9, 1309, (2019).
- [10] M.S. Niasari, F. Davar, M. Mazaheri, *Mater. Lett.* 62, (1890–1892), (2008).
- [11] M.S. Takumoto, S.H. Pulcinelli, C.V. Santilli, V. Briois, *J. Phys. Chem.* 107, 568, (2003).
- [12] J. Zhou, F. Zhao, Y. Wang, Y. Zhang, L. Yang, *J. Lumin.* (122–123), (195–197), (2007).
- [13] H.J. Zhai, W.H. Wu, F. Lu, H.-S. Wang, C. Wang, *Mater. Chem. Phys.* 112, (1024–1028), (2008).

- [14] M. Bitenc, M. Marinsek, Z. Crnjak Orel, J. Eur. Ceram. Soc. 28, (2915–2921), (2008).
- [15] K. Okuyama, I.W. Lenggoro, Chem. Eng. Sci. 58 (537–547), (2003).
- [16] D. Cao, S. Gong, S. Liang, Nanoscale Research Letters 14, 210, (2019).
- [17] S. V. Reddy, S. Peyyala, Asian Journal of Nanoscience and materials, 2, (111-119), (2019).
- [18] K.S. Suslick, S.B. Choe, A.A. Cichowlas, M.W. Grinstaff, Nature 353, (414), (1991).
- [19] H. Wang, J.J. Zhu, J.M. Zhu, H.Y. Chen, J. Phys. Chem. 106, (3848), (2002).
- [20] S.I. Nikitenko, Yu. Koltypin, A. Gedanken, J. Mater. Chem. 12, (1107), (2002).
- [21] K.S. Suslick, M. Fang, T. Hyeon, J. Am. Chem. Soc. 118, (11960), (1996).
- [22] M. S. Niasari, G. Hosseinzadeh, F. Davar, Journal of Alloys and Compounds, 509, (134–140), (2011).
- [23] M. Sugimoto, J. Magn, Chem. Mater. 133, (460), (1994).
- [24] M. Martos, J. Morales, L. Sanchez, R. Ayouchi, D. Leinen, F. Martin, J.R. Ramos Barrado, Electrochimica Acta 46, (2939), (2001).
- [25] S. Sudarmonoharan, M.L. Rao, Sonochemical synthesis of nanomaterials, in: H.S. Nalwa (Eds.), "Encyclopedia of Nanoscience and Nanotechnology", American Scientific Publishers, vol. 10, (67–82), (2004).
- [26] B. D. Cullity, "Elements of x-ray diffraction", (Addison-Wesley publishing company, Inc., California, Vol. 1, (531), (1956).
- [27] M. S. Niasari, F. Davar, M. Mazaheri, M. Shaterian, J. Magn. Mater. 320, (575–578), (2008).
- [28] M. Birkholz, "Thin Film Analysis by X-ray Scattering", Wiley-VCH Verlag GmbH and Co. KGaA, Weinheim, Vol 1, 378, (2006).
- [29] A. Hernández, L. Maya, E. S. Mora and E. M. Sánchez, J Sol-Gel Sci Techn, 42, (71-78), (2007).
- [30] JR. Ferraro, "Low frequency vibrations of inorganic and co-ordination compounds", Plenum Press, New York, 309 (1971).
- [31] T. Lopez, J. Mendez, T. Zamudio, M. Villa, Mater Chem Phys 30, (161-167), (1992).
- [32] N.F. Mott and E.A. Davis, "Electronic processes in non-crystalline materials", Clarendon Press (Oxford and New York) 2nd ed, (590), (1979).
- [33] E.A. Davis, and N.F. Mott, "Conduction in non-crystalline systems V. Conductivity, optical absorption and photoconductivity in amorphous semiconductors", Philosophical Magazine, 22, (903), (1970).
- [34] L.I. Berger, Semiconductor Materials, CRC, Boca Raton, Fla, USA, 122, (472), (1997).

### توصيف أكسيد الزنك النانومتري المحضر باستخدام الطريقة السونوكيميائية بتغيير قدرات الاكتراسونيك المعرض لها

مصطفى عبدالله عشوش<sup>1</sup>، لبنى الصباح<sup>3</sup>، احمد محمد عيد<sup>4</sup>، سوزان ناصر السيد<sup>2</sup>، اسماء عبد الغني عماره<sup>4</sup>

<sup>1</sup> كلية العلوم – جامعة الازهر – القاهرة – مصر، <sup>2</sup> كلية العلوم فرع البنات – جامعة الازهر – القاهرة، <sup>3</sup> المعهد العالي للتكنولوجيا – فرع السادس من اكتوبر -مدينة 6 اكتوبر- القاهرة، <sup>4</sup> المعهد القومي للمعايرة – شارع ترسا - الجيزة – القاهرة

1. تناولت هذه الدراسة تحضير أكسيد الزنك النانومتري باستخدام الطريقة السونوكيميائية وهي طريقة تعتمد علي تعريض المحاليل للكيميائية للموجات فوق صوتية (الأتراسونيك).
2. تم تحضير ثلاث عينات مختلفة من أكسيد الزنك تختلف في قيمة القدرة للموجات فوق صوتية المستخدمة في تحضير كل عينة.
3. تم التحضير عند نسب من القدرة تساوي 20% و 40% و 60% من القدرة الكلية لجهاز السونوفير (الجهاز المولد للموجات الصوتية).
4. تم استخدام حيود الأشعة السينية في دراسة الحجم الجسيمي ومعامل الانضغاطية (ε) وذلك بتطبيق معادلة شيرر واستخدام تحليل ويليمسن- هول (Williamson-Hall Analysis) وقد توافقت النتائج معاً
5. كذلك توافقت قيم الحجم الجسيمي المحسوبة من حيود الأشعة السينية مع القيم المقاسة باستخدام الميكروسكوب الالكتروني.
6. وقد أظهرت صور الميكروسكوب الالكتروني تغيير في المورفولوجي بتغيير قدرة الموجات الصوتية التي يتم تعريضها للمحلول أثناء التحضير.
7. تم قياس الخواص الضوئية للعينات الثلاث باستخدام طيف الأشعة تحت الحمراء (FTIR) وأوضحت النتائج وجود شريط الامتصاص المميز لأكسيد الزنك بالقرب من 650 سم<sup>-1</sup>.
8. وللحصول علي معلومات عن قيمة حاجز الجهد فقد تم قياس طيف الامتصاص والانبعث في المدى

النانونمتری (200 – 800 نانومتر) ووجد أنه  
يساوی 3.1 الكترون فولت.